Inorg. Chem. **2003**, *42*, 3751–3764

Influences of Changes in Multitopic Tris(pyrazolyl)methane Ligand Topology on Silver(I) Supramolecular Structures

Daniel L. Reger,*,† Radu F. Semeniuc,† Ioan Silaghi-Dumitrescu,‡ and Mark D. Smith†

Department of Chemistry and Biochemistry, University of South Carolina, Columbia, South Carolina 29208, and Facultatea de Chimie şi Inginerie Chimică, Universitatea Babeş-Bolyai, Cluj-Napoca, Romania

Received January 15, 2003

The reactions between silver tetrafluoroborate and the ligands 1,2,4,5-$C_6H_2[CH_2OCH_2C(pz)_3]_4$ (**L1**, pz = pyrazolyl ring), *o*-$C_6H_4[CH_2OCH_2C(pz)_3]_2$ (**L2**), and *m*-$C_6H_4[CH_2OCH_2C(pz)_3]_2$ (**L3**) yield coordination polymers of the formula $\{C_6H_{6-n}[CH_2OCH_2C(pz)_3]_n(AgBF4)_m\}_\infty$ ($n = 4$, $m = 2$, **1**; $n = 2$, *ortho* substitution, $m = 1$, **2**; *meta* substitution, $m = 2$, **3**). In the solid state, **L2** molecules dimerize by a pair of C–H···π interactions, forming an arrangement that resembles the tetratopic ligand **L1**. In the solid-state structure of **1**, each silver atom is κ^2-bonded to two tris(pyrazolyl)methane units from different ligands with the overall structure a polymer made up from 32-atom macrocyclic rings formed by bonding tris(pyrazolyl)methane groups from nonadjacent positions on the central arene rings to the same two silver atoms. In **2**, each silver is bonded to two tris(pyrazolyl)methane units in the same κ^2–κ^2 fashion as with **1**, forming a polymer chain. The chains are organized into dimeric units by strong face-to-face π–π stacking between the central arene rings making bitopic **L2** act as half of tetratopic **L1**. The chains in both structures are organized by weak C–H···F hydrogen bonds and π–π stacking interactions into very similar 3D supramolecular architectures. The structure of **3** contains three types of silvers with the overall 3D supramolecular sinusoidal structure comprised of 32-atom macrocycles. Infrared studies confirm the importance of the noncovalent interactions. Calculations at the DFT (B3LYP/6-31G*) level of theory have been carried out on **L2** and also support C–H···π interactions. Electrospray mass spectral data collected from acetone or acetonitrile show the presence of aggregated species such as $[(L)Ag_2(BF_4)]^+$ and $[(L)Ag_2]^{2+}$, despite the fact that ^{1}H NMR spectra of all compounds show that acetonitrile completely displaces the ligand whereas acetone does not.

Introduction

Investigations into the architecture of supramolecular compounds formed by the self-assembly processes have been ongoing in the last two decades.[1] A growing field in this area is the synthesis and characterization of coordination polymers showing a number of infinite 1-D, 2-D, and 3-D structures with specific geometries and properties.[2] The key features that determine the overall structures of coordination polymers are the ligand topicity (i.e. the positions of coordinating groups), flexibility or rigidity of the linker groups joining the coordination sites, and the stereochemical preferences of the coordinated metal ion.[1b−f,3] The role of noncovalent interactions is also recognized as providing further organization into more complex networks. A wide

* To whom correspondence should be addressed. Reger@mail.chem.sc.edu.

† University of South Carolina.

‡ Universitatea Babeş-Bolyai.

(1) (a) Piguet, C.; Bernardinelli, G.; Hopfgartner G. *Chem. Rev.* **1997**, *97*, 2005. (b) Hagrman, P. J.; Hagrman, D.; Zubieta, J. *Angew. Chem., Int. Ed.* **1999**, *38*, 2638. (c) Khlobystov, A. N.; Blake, A. J.; Champness, N. R.; Lemenovskii, D. A.; Majouga, G.; Zyk, N. V.; Schroder, M. *Coord. Chem. Rev.* **2001**, *222*, 155. (d) Blake, A. J.; Champness, N. R.; Hubberstey, P.; Li, W. S.; Withersby, M. A.; Schroder, M. *Coord Chem. Rev.* **1999**, *183*, 117. (e) Batten, S. T.; Robson, R. *Angew. Chem., Int. Ed.* **1998**, *37*, 1461. (f) Nguyen, P.; Gomez-Elipe, P.; Manners, I. *Chem. Rev.* **1999**, *99*, 1515. (g) Leininger, S.; Olenyuk, B.; Stang, P. J. *Chem. Rev.* **2000**, *100*, 853. (h) Swiegers, G. F.; Malefetse, T. J. *Chem. Rev.* **2000**, *100*, 3483. (i) Seidel, R. S.; Stang, P. J. *Acc. Chem. Res.* **2002**, *35*, 972. (j) Zaworotko, M. J. *Chem. Commun.* **2001**, 1.

(2) (a) Gardner, G. B.; Venkataraman, D.; Moore, J. S.; Lee, S. *Nature* **1995**, *374*, 792−793. (b) Venkataraman, D.; Gardner, G. B.; Lee, S.; Moore J. S. *J. Am. Chem. Soc.* **1995**, *117*, 11600−11601. (c) Yaghi, O. M.; Li, G.; Li, H. *Nature* **1995**, *378*, 703−706. (d) Hennigar, T. J.; MacQuarrie, D. C.; Losier, P.; Rogers, R. D.; Zaworotko, M. J. *Angew. Chem., Int. Ed. Engl.* **1997**, *36*, 972. (e) Müller, I. M.; Röttgers, T.; Sheldrik, W. S. *Chem. Commun.* **1998**, 823. (f) Hong, M.; Zhao, Y.; Su, W.; Cao, R.; Fujita, M.; Zhou, Z.; Chan, A. S. C. *Angew. Chem., Int. Ed.* **2000**, *39*, 2468. (g) Blake, A. J.; Champness, N. R.; Cooke, P. A.; Nicolson, J. E. B. *Chem. Commun.* **2000**, 665.

10.1021/ic034039r CCC: $25.00
Published on Web 05/15/2003

variety of these interactions, some relating to the anions[3a−d,4] and the solvent,[2g,3b,5] was found to have an impact on the crystal packing of several compounds. Important examples are strong[6] and weak[3e,7] hydrogen bonds, $\pi-\pi$ stacking,[8] X−H···π interactions (X = O, N, C),[9] and interhalogen interactions.[10]

How these organizational features determine supramolecular structures still needs to be clearly elucidated.[11,12] Our efforts in this area are based on the chemistry of metal complexes of tris(pyrazolyl)methane ligands (Chart 1),[13] potentially tripodal, neutral ligand sets isoelectronic to the more heavily studied tris(pyrazolyl)borate ligands.[14] We have recently reported substantial improvements in the preparations of tris(pyrazolyl)methane ligands[15] and developed chemistry of them where the central methine carbon atom can be fuctionalized with groups other than a hydrogen atom.[15e] Using this chemistry, we have prepared multitopic ligands of the general formula $C_6H_{6-n}[CH_2OCH_2C(pz)_3]_n$ (n = 2, 4, pz = pyrazolyl ring).[16] We have reported that the reaction of the three isomers *ortho*-, *meta*-, and *para*-$C_6H_4[CH_2OCH_2C(pz)_3]_2$ with $[Cd_2(thf)_5](BF_4)_4$ leads to the formation of coordination polymers of the formula {$C_6H_4[CH_2$-

Chart 1. Tris(pyrazolyl)methane

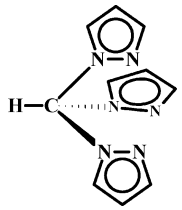

(3) (a) Hirsch, K. A.; Wilson, S. R.; Moore, J. S. *Inorg. Chem.* **1997**, *36*, 2960. (b) Blake, A. J.; Champness, N. R.; Cooke, P. A.; Nicolson J. E. B.; Wilson C. *J. Chem. Soc., Dalton Trans*. **2000**, 3811. (c) Yang, S.-P.; Chen, X.-M.; Ji, L. *J. Chem. Soc., Dalton Trans*. **2000**, 2337. (d) Fei, B.-L., Sun, W.-Y., Yu, K-.B., Tang, W.-X. *J. Chem. Soc., Dalton Trans*. **2000**, 805. (e) Paul, R. L.; S. M. Couchman, S. M.; Jeffery, J. C.; McCleverty, J. A.; Reeves, Z. R.; Ward, M. D. *J. Chem. Soc., Dalton Trans.* **2000**, 845. (f) Carlucci, L.; Ciani, G.; Proserpio, D. M.; Rizzato, S. *Cryst. Eng. Comm*. **2002**, *4*, 121. (g) Plater, J. M.; Foreman, M. R. St. J.; Slawin, A. M. *J. Chem. Res., Synop*. **1999**, *74*. (h) Carlucci, L.; Ciani, G.; Proserpio, D. M.; Rizzato, S. *Cryst. Eng. Comm.* **2002**, *4*, 431.

(4) (a) Withersby, M. A.; Blake, A. J.; Champness, N. R.; Hubberstey, P.; Li W.-S.; Schröder, M. *Angew. Chem., Int. Ed. Engl.* **1997**, *36*, 2327. (b) Vilar, R.; Mingos, D. M. P.; White, A. J. P.; Williams, D. J. *Angew. Chem., Int. Ed.* **1998**, *37*, 1258. (c) Hong, M. C.; Su, W. P.; Cao, R.; Fujita, M.; Lu, J. X. *Chem. Eur. J.* **2000**, *6*, 427.

(5) (a) Withersby, M. A.; Blake, A. J.; Champness, N. R.; Cooke, P. A. Hubberstey, P.; Li, W.-S.; Schröder, M. *Inorg. Chem.* **1999**, *38*, 2259. (b) Subramanian, S.; Zaworotko, M. J. *Angew. Chem., Int. Ed. Engl.* **1995**, *34*, 2127. (c) Lu, J.; T. Paliwala, T.; Lim, S. C.; Yu, C.; Niu, T.; Jacobson, A. J. *Inorg. Chem.* **1997**, *36*, 923.

(6) Strong hydrogen bonds include interactions of the type O−H···O, N−H···O, O−H···N, and N−H···N. See for example: (a) Braga, D.; Grepioni, F. J. *Chem. Soc, Dalton Trans*. **1999**, 1. (b) Allen, M. T.; Burrows, A. D.; Mahon, M. F. *J. Chem. Soc, Dalton Trans*. **1999**, 215. (c) Ziener, U.; Breuning, E.; Lehn, J.-M.; Wegelius, E.; Rissanen, K.; Baum, G.; Fenske, D.; Vaughan, G. *Chem. Eur. J*. **2000**, *6*, 4132. (d) Goddard, R.; Claramunt, R. M. Escolastico, C.; Elguero, J. *New. J. Chem.* **1999**, 237.

(7) A weak hydrogen bond (X−H···Y) involves less electronegative atoms; we discuss here only the C−H···Y type of weak hydrogen bond (Y = O, F). See for example: (a) Calhorda, M. J. *Chem. Commun*. **2000**, 801. (b) Desiraju, G. R. *Acc. Chem. Res.* **1996**, *29*, 441. (c) Grepioni, F.; Cojazzi, G.; Draper, S. M.; Scully, N.; Braga, D. *Organometallic*s **1998**, *17*, 296. (d) Weiss, H. C.; Boese, R.; Smith, H. L.; Haley, M. M. *Chem. Commun*. **1997**, 2403.

(8) Janiak, C. *J. Chem. Soc., Dalton Trans*. **2000**, 3885 and references therein.

(9) (a) Takahashi, H.; Tsuboyama, S.; Umezawa, Y.; Honda, K.; Nishio, M. *Tetrahedron* **2000**, *56*, 6185. (b) Tsuzuki, S.; Honda, K.; Uchimaru, T.; Mikami, M.; Tanabe, K. *J. Am. Chem. Soc.* **2000**, *122*, 11450. (c) Seneque, O.; Giorgi, M.; Reinaud, O. *Chem. Commun*. **2001**, 984. (d) Weiss, H. C.; Blaser, D.; Boese, R.; Doughan, B. M.; Haley, M. M. *Chem. Commun.* **1997**, 1703. (e) Madhavi, N. N. L.; Katz, A. K.; Carrell, H. L.; Nangia, A.; Desiraju, G. R. *Chem. Commun*. **1997**, 2249. (f) Madhavi, N. N. L.; Katz, A. K.; Carrell, H. L.; Nangia, A.; Desiraju, G. R. *Chem. Commun*. **1997**, 1953. (g) Nishio, M.; Hirota, M.; Umezawa, Y. *The CH/π Interaction Evidence, Nature and Consequences*; Wiley-VCH: New York, 1998.

(10) (a) Reddy, D. S.; Craig, D. C.; Desiraju, G. R. *J. Am. Chem. Soc.* **1996**, 118, 4090. (b) Kowalik, J.; VanDerveer, D.; Clower, C.; Tolbert, L. M. *Chem. Commun*. **1999**, 2007. (c) Freytag, M.; Jones, P. G.; Ahrens, B.; Fischer, A. K. *New J. Chem*. **1999**, *23*, 1137. (d) Ram Thaimattam, R.; Reddy, D. S.; Xue, F.; Mak, T. C. W.; Nangia, A.; Desiraju, G. R. *New J. Chem*. **1998**, *22*, 143.

(11) (a) Desiraju, G. R. *Angew. Chem., Int. Ed. Engl.* **1995**, *34*, 2311. (b) Blake, A. J.; Baum, G.; Champness, N. R.; Chung, S. S. M.; Cooke, P. A.; Fenske, D.; Khlobystov, A. N.; Lemenovskii, D. A.; Li, W.-S.; Schroder, M. *J. Chem. Soc., Dalton Trans*. **2000**, 4285.

(12) (a) Reddy, D. S.; Ovchinnikov, Y. E.; Shishkin, O. V. Struchkov, Y. T.; Desiraju, G. R. *J. Am. Chem. Soc.* **1996**, *118*, 4085. (b) Allen, F. H.; Hoy, V. J.; Howard, J. A. K.; Thalladi, V. R.; Desiraju, G. R.; Wilson, C. C.; McIntyre, G. J. *J. Am. Chem. Soc.* **1997**, *119*, 3477−3480. (c) Thaimattam, R.; Xue, F.; Sarma, J. A. R. P.; Mak, T. C. W.; Desiraju, G. R. *J. Am. Chem. Soc.* **2001**, *123*, 4432. (d) Kuduva, S. S.; Craig, D. C.; Nangia; A.; Desiraju, G. R. *J. Am. Chem. Soc.* **1999**, *121*, 1936−1944.

(13) (a) Reger, D. L.; Collins, J. E.; Rheingold, A. L.; Liable-Sands, L. M. *Organometallics* **1996**, *15*, 2029. (b) Jameson, D. L.; Castellano, R. K. *Inorg. Synth.* **1998**, *32*, 51. (c) Titze, C.; Hermann, J.; Vahrenkamp, H. *Chem. Ber.* **1995**, *118*, 1095. (d) Reger, D. L.; Collins, J. E.; Layland, R.; Adams, R. D. *Inorg. Chem.* **1996**, *35*, 1372. (e) Reger, D. L.; Collins, J. E.; Matthews, M. A.; Rheingold, A. L.; Liable-Sands, L. M.; Guzei, I. A. *Inorg. Chem.* **1997**, *36*, 6266. (f) Reger, D. L.; Collins, J. E.; Rheingold, A. L.; Liable-Sands, L. M.; Yap, G. P. A. *Inorg. Chem.* **1997**, *36*, 345. (g) Reger, D. L. *Comments Inorg. Chem.* **1999**, *21*, 1. (h) Reger, D. L.; Little, C. A.; Rheingold, A. L.; Lam, M.; Concolino, T.; Mohan, A.; Long, G. J. *Inorg. Chem.* **2000**, *39*, 4674. (i) Reger, D. L.; Little, C. A.; Rheingold, A. L.; Lam, M.; Liable-Sands, L. M.; Rhagitan, B. M.; Concolino, T.; Mohan, A.; Long, G. J.; Briois, V.; Grandjean, F. *Inorg. Chem.* **2001**, *40*, 1508. (j) Byers, P. K.; Canty, A. J.; Honeyman, R. T. *Adv. Organomet. Chem.* **1992**, *34*, 1.

(14) (a) Trofimenko, S. *Acc. Chem. Res*. **1971**, *4*, 17. (b) Trofimenko, S. *J. Am. Chem. Soc*. **1967**, *89*, 3170. (c) Trofimenko, S. *J. Am. Chem. Soc*. **1967**, *89*, 6288. (d) Shaver, A. J. *Organomet. Chem. Libr*. **1976**, *3*, 157. (e) Trofimenko, S. *Prog. Inorg. Chem.* **1988**, *34*, 115. (f) Trofimenko, S. *Chem. Rev.* **1993**, *93*, 943. (g) Trofimenko, S.; Calabrese, J. C.; Thompson, J. S. *Inorg. Chem.* **1987**, *26*, 1507. (h) Trofimenko, S. *Scorpionates-The Coordination Chemistry of Poly-(pyrazolyl)borate Ligands*; Imperial College Press: London, 1999. (i) Lipton, A. S.; Mason, S. S.; Myers, S. M.; Reger, D. L.; Ellis, P. D. *Inorg. Chem.* **1996**, *35*, 7111. (j) Reger, D. L.; Myers, S. M.; Mason, S. S.; Darensbourg, D. J.; Holtcamp, M. W.; Reibenspeis, J. H.; Lipton, A. S.; Ellis, P. D. *J. Am. Chem. Soc.* **1995**, *117*, 10998. (k) Reger, D. L.; Myers, S. M.; Mason, S. S.; Rheingold, A. L.; Haggerty, B. S.; Ellis, P. D. *Inorg. Chem.* **1995**, *34*, 4996. (l) Reger, D. L.; Mason, S. S.; Rheingold, A. L. *Inorg. Chim. Acta* **1995**, *240*, 669. (m) Lipton, A. S.; Mason, S. S., Reger, D. L.; Ellis, P. D. *J. Am. Chem. Soc.* **1994**, *116*, 10182.

(15) (a) Reger, D. L.; Collins, J. E.; Jameson, D. L.; Castellano, R. K. *Inorg. Synth.* **1998**, *32*, 63. (b) Reger, D. L.; Collins, J. E.; Rheingold, A. L.; Liable-Sands, L. M.; Yap, G. P. A. *Organometallics* **1997**, *16*, 349. (c) Reger, D. L.; Collins, J. E.; Myers, S. M.; Rheingold, A. L.; Liable-Sands, L. M. *Inorg. Chem.* **1996**, *35*, 4904. (d) Reger, D. L.; Grattan, T. C.; Brown, K. J.; Little, C. A.; Lamba, J. J. S.; Rheingold, A. L.; Sommer, R. D. *J. Organomet. Chem.* **2000**, *607*, 120. (e) Reger, D. L.; Grattan, T. C. *Synthesis* **2003**, 350.

(16) (a) Reger, D. L.; Wright, T. D.; Semeniuc, R. F.; Grattan T. C.; Smith, M. D. *Inorg. Chem.* **2001**, *40*, 6212. (b) Reger, D. L.; Semeniuc, R. F.; Smith, M. D. *Inorg. Chem.* **2001**, *40*, 6545. (c) Reger, D. L.; Semeniuc, R. F.; Smith, M. D. *Eur. J. Inorg. Chem.* **2002**, 543. (d) Reger, D. L.; Semeniuc, R. F.; Smith, M. D. *J. Chem. Soc., Dalton Trans*. **2002**, 476. (e) Reger, D. L.; Semeniuc, R. F.; Smith, M. D. *Inorg. Chem. Commun*. **2002**, *5*, 278. (f) Reger, D. L.; Semeniuc, R. F.; Smith, M. D. *J. Organomet. Chem*. **2003**, *666*, 87. (g) Reger, D. L.; Semeniuc, R. F.; Smith, M. D. *J. Chem. Soc., Dalton Trans*. **2003**, 285.

Chart 2. Possible Modes of Coordination of Tris(pyrazolyl)methane Units to Silver(I) Metal Centers

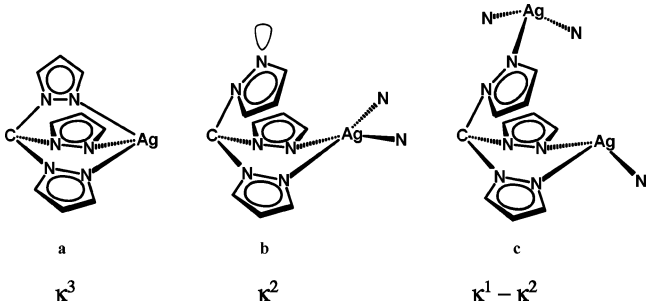

$OCH_2C(pz)_3]_2Cd\}(BF_4)_2\}_n$, each with a different supramolecular structure even though they had the same octahedral coordination environment about the cadmium.[16a] We have also shown that metal complexes of these ligands form 2-D and 3-D supramolecular structures organized by a multitude of noncovalent interactions, such as weak hydrogen bonds[16a−d] and intermolecular[16b,f] or intramolecular[16d,f] $\pi-\pi$ stacking and C−H···π interactions.[16b,f,g] In addition, in some cases, the metal complexes of these ligands undergo an interesting double $\pi-\pi$/C−H···π interaction.[16f] This versatility is a consequence of the presence of the aromatic pyrazolyl rings and linking arene rings that can act as acceptors in C−H···π interactions or participate in $\pi-\pi$ stacking. Another factor is the hydrogen atoms within the pyrazolyl rings are acidic enough to be involved in weak hydrogen bonds. In addition, the tris(pyrazolyl)methane units can act as (a) κ^3 tripodal, (b) κ^2 bonded to a single metal with the third pyrazolyl not coordinated, and (c) $\kappa^1-\kappa^2$ bonded bridging two metals (Chart 2).

These bonding features were anticipated for ligands that were designed to use the versatile bonding properties of tris(pyrazolyl)methane units coupled with a semirigid linker, intermediate between rigid ligands[1c,d] and more flexible ligands[3f−h] used by others. The supramolecular structures of rigid ligand complexes are dominated by covalent interactions, and noncovalent forces have little effect upon network topology.[1d,e] This organization with rigid ligands allows a better prediction of the overall structure, shape, and porosity of the resulting array, and therefore, they have been widely used. In contrast, the use of flexible ligands in the construction of supramolecular arrays has been less systematic, due to the lack of predictability of the structural outcome of the covalent and/or supramolecular network. The semirigid ligands used in our studies can adjust their shape to maximize covalent and noncovalent interactions, and the overall structure of the supramolecular array will be the resultant of the interplay among all forces. The rigid central arene ring and the tris(pyrazolyl)methane units offer structure to the system, while the flexible ether-based linkages offer versatility to the system and improve the solubility of the coordination polymers.

In an attempt to elucidate the intimate processes that lead to the formation of supramolecular species based on these ligands and to analyze the competition between covalent and noncovalent interactions, we report here the results of reactions of $AgBF_4$ with ligands **L1**, **L2**, and **L3** (Chart 3).

Chart 3

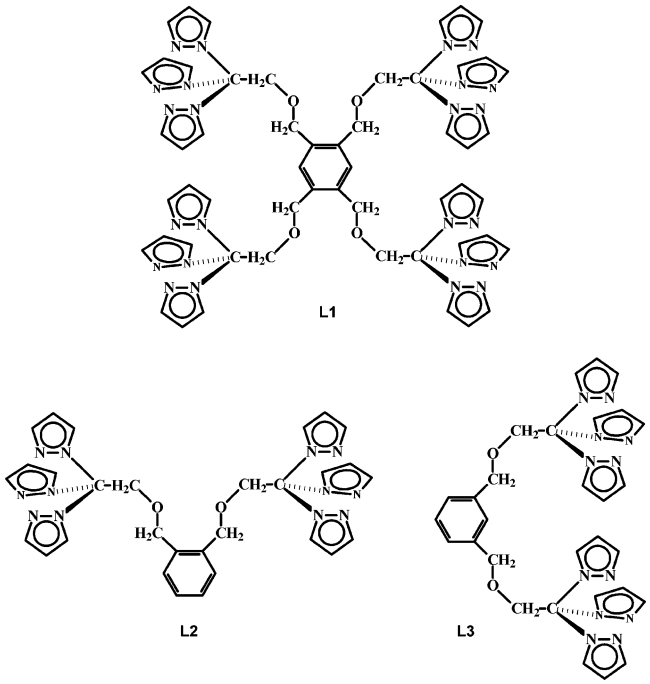

The tetratopic ligand **L1** has four tris(pyrazolyl)methane units linked to a central arene ring via four ether-based sidearms in the 1,2,4,5-positions. As can be seen in Chart 3, both **L2** and **L3** can be considered as "half" of **L1**, each containing two identical sidearms in the 1,2- and 1,3-positions, respectively, connected to a central arene ring. This investigation is (to the best of our knowledge) the first systematic study on how designed changes in ligand toplogy with systems consisting of semirigid ligands will influence the outcome of the covalent and noncovalent networks. We have communicated the structure of **1** previously.[16b]

Experimental Section

General Procedure. All operations were carried out under a nitrogen atmosphere using standard Schlenk techniques and a Vacuum Atmospheres HE-493 drybox. All solvents were dried and distilled prior to use. The ^{1}H NMR spectra were recorded on a Varian AM300 spectrometer using a broad-band probe. Proton chemical shifts are reported in ppm vs internal Me_4Si. IR spectra were recorded on a Nicolet 5DXBO FTIR spectrometer. Electrospray ionization mass spectrometry data were obtained on a MicroMass QTOF spectrometer. Clusters assigned to specific ions show appropriate isotopic patterns as calculated for the atoms present. Elemental analyses were performed by Robertson Microlit Laboratories (Madison, NJ). 2,2,2-Tris(1-pyrazoyl)ethanol, $HOCH_2C(pz)_3$,[15c,e] and the ligands **L1**,[16f] **L2**, and **L3**[16a] were prepared by following literature methods.

$\{1,2,4,5\text{-}C_6H_2[CH_2OCH_2C(pz)_3]_4(AgBF_4)_2\}_\infty$ (1). $1,2,4,5\text{-}C_6H_2[CH_2OCH_2C(pz)_3]_4$, **L1** (0.22 g, 0.20 mmol), was dissolved in thf (25 mL). This solution was added dropwise to a solution of silver tetrafluoroborate, $AgBF_4$ (0.078 g, 0.40 mmol), in dry thf (15 mL) under an inert atmosphere. A white precipitate appeared as the mixture was stirred for 2 h. The thf was removed by cannula filtration; the white precipitate washed with thf (2 × 10 mL) and then vacuum-dried to afford 0.226 g (73.8%) of solid identified as $\{C_6H_2[CH_2OCH_2C(pz)_3]_4Ag_2(BF_4)_2)\}_\infty$. ^{1}H NMR (acetone-$d_6$): δ

Table 1. Crystallographic Data and Structure Refinement for $\{1,2,4,5\text{-}C_6H_2[CH_2OCH_2C(pz)_3]_4(AgBF_4)_2\}_\infty$ (**1**), $\{o\text{-}C_6H_4[CH_2OCH_2C(pz)_3]_2(AgBF_4)\}_\infty$ (**2**), and $\{m\text{-}C_6H_4[CH_2OCH_2C(pz)_3]_2(AgBF_4)_2\}_\infty$ (**3**)

	1	**2**	**3**
empirical formula	$C_{62}H_{66}Ag_2B_2F_8N_{28}O_4$	$C_{32}H_{35}AgBF_4N_{12}O_{2.50}$	$C_{31}H_{33}Ag_2B_2F_8N_{13}O_4$
fw	1656.79	822.40	1041.06
temp, K	173(2)	173(2)	190(2)
crystal system	triclinic	monoclinic	monoclinic
space group	$P\bar{1}$	$C2/c$	$P2/c$
a, Å	11.4424(19)	28.606(2)	10.9226(7)
b, Å	11.972(2)	14.9439(11)	13.1641(8)
c, Å	13.962(2)	17.2648(13)	27.1563(18)
α, deg	106.838(3)	90	90
β, deg	92.871(3)	109.778(2)	95.519(2)
γ, deg	100.803(3)	90	90
V, Å^3	1787.1(5)	6945.0(9)	3886.6(4)
Z	1	8	4
D(calcd), Mg m^{-3}	1.539	1.573	1.779
abs coeff, mm^{-1}	0.637	0.654	1.102
F(000)	842	3352	2072
cryst size, mm	0.56 × 0.32 × 0.18	0.36 × 0.16 × 0.06	0.10 × 0.08 × 0.04
reflcns collcd	12 727	22 836	18 040
indpdt reflcns	6285 [R(int) = 0.0200]	7104 [R(int) = 0.0366]	5603 [R(int) = 0.0993]
data/restraints/params	6285/0/480	7104/0/475	5603/6/599
goodness-of-fit on F^2	1.008	1.004	1.013
final R indices [$I > 2\sigma(I)$]	R1 = 0.0374, wR2 = 0.0977	R1 = 0.0402, wR2 = 0.0901	R1 = 0.0527, wR2 = 0.0868
R indices (all data)	R1 = 0.0455, wR2 = 0.1005	R1 = 0.0607, wR2 = 0.0973	R1 = 0.1054, wR2 = 0.1067

7.75, 7.66 (d, d, J = 1.5 Hz, J = 2.4 Hz, 12,12 H, 3,5-H pz), 7.40 (s, 2 H, C_6H_2), 6.53 (dd, J = 1.6, 2.4 Hz, 12 H, 4-H pz), 4.99 (s, 8 H, OCH_2C(pz)$_3$), 4.43 (s, 8 H, OCH_2Ph). ES$^+$/MS (m/z): $[C_{54}H_{54}N_{24}O_4BF_4Ag_2]^+$ calcd 1403.2900; found 1403.2877. Anal. Calcd for $C_{54}H_{54}Ag_2B_2F_8N_{24}O_4$: C, 43.46; H, 3.65. Found: C, 43.21; H, 3.48.

$\{o\text{-}C_6H_4[CH_2OCH_2C(pz)_3]_2(AgBF_4)\}_\infty$ (2). This compound was prepared as above for **1** using o-$C_6H_4[CH_2OCH_2C(pz)_3]_2$, **L2** (0.295 g, 0.50 mmol), and $AgBF_4$ (0.0975 g, 0.50 mmol) to yield 0.282 g (72%) of solid identified as $\{o\text{-}C_6H_4[CH_2OCH_2C(pz)_3]_2(AgBF_4)\}_\infty$. ^{1}H NMR (acetone-$d_6$): δ 7.88, 7.55 (d, d, J = 1.5 Hz, J = 2.7 Hz, 6, 6 H, 3,5-H pz), 7.30−7.25 (m, 4 H, C_6H_4), 6.53 (dd, J = 1.7, 2.7 Hz, 6 H, 4-H pz), 5.22 (s, 4 H, OCH_2C(pz)$_3$), 4.54 (s, 4 H, OCH_2Ph). ES$^+$/MS (m/z): $[C_{30}H_{30}N_{12}O_2Ag]^+$ calcd 697.1666; found 697.1677. Anal. Calcd for $C_{30}H_{30}AgBF_4N_{12}O_2$: C, 45.88; H, 3.85. Found: C, 45.56; H, 4.12.

$\{m\text{-}C_6H_4[CH_2OCH_2C(pz)_3]_2(AgBF_4)_2\}_\infty$ (3). This compound was prepared as above for **1** using m-$C_6H_4[CH_2OCH_2C(pz)_3]_2$, **L3** (0.295 g, 0.50 mmol), and $AgBF_4$ (0.195 g, 1.0 mmol) to yield 0.341 g (70%) of solid identified as $\{m\text{-}C_6H_4[CH_2OCH_2C(pz)_3]_2(AgBF_4)_2\}_\infty$. ^{1}H NMR (acetone-$d_6$): δ 7.75, 7.64 (d, d, J = 1.5 Hz, J = 2.7 Hz, 6, 6 H, 3,5-H pz), 7.32−7.14 (m, 4 H, C_6H_4), 6.53 (dd, J = 1.7, 2.7 Hz, 6 H, 4-H pz), 5.21 (s, 4 H, OCH_2C(pz)$_3$), 4.65 (s, 4 H, OCH_2Ph). ES$^+$/MS (m/z): $[C_{30}H_{30}N_{12}O_2Ag]^+$ calcd 697.1666; found 697.1681. Anal. Calcd for $C_{30}H_{30}Ag_2B_2F_8N_{12}O_2$: C, 36.77; H, 3.09. Found: C, 37.01; H, 2.98.

X-ray Structural Studies. Crystals for compounds **1** and **2** were grown from acetonitrile by vapor phase diffusion of diethyl ether, and crystals for compound **3,** from nitromethane using the same method of crystallization. Suitable colorless single crystals of **1**−**3** were selected and mounted onto thin glass fibers. Low-temperature X-ray intensity data were measured on a Bruker SMART APEX CCD-based diffractometer (Mo Kα radiation, λ = 0.710 73 Å). After preliminary crystal quality and unit cell parameter determination, a full sphere (**1**) or hemisphere (**2**, **3**) of raw frame data was collected. Raw data frame integration was performed with SAINT+,[17] which also applied corrections for Lorentz and polarization effects. Analysis of each data set showed negligible crystal decay during data collection. Empirical absorption corrections were applied to each data set (SADABS).[18] The reported final unit cell parameters are based on the least-squares refinement of all reflections from each data set with $I > 5\sigma(I)$. The structures were solved by a combination of direct methods and difference Fourier syntheses and refined by full-matrix least-squares against F^2 (SHELXTL).[18] Non-hydrogen atoms in each structure were refined with anisotropic displacement parameters; hydrogen atoms were placed in idealized positions and included as riding atoms. **1** crystallizes in the triclinic space group $P\bar{1}$. The centroid of the arene ring of the ligand lies on an inversion center. The asymmetric unit contains one Ag atom, half a ligand, one BF_4^- counterion, and two acetonitrile molecules of crystallization. Systematic absences in the intensity data for **2** indicate the monoclinic space groups Cc or $C2/c$, the latter of which was confirmed. The asymmetric unit consists of a silver atom, an *ortho*-$C_{30}H_{30}N_{12}O_2$ ligand, a BF_4^- counterion and half of a diethyl ether molecule located on a 2-fold axis of rotation. Systematic absences in the intensity data for **3** were consistent with the monoclinic space groups Pc and $P2/c$, the latter of which was confirmed. The asymmetric unit contains three crystallographically independent Ag atoms: Ag1, which resides on a 2-fold rotational axis; Ag2, on a general position; Ag3, located on a center of symmetry. One complete *meta*-$C_{30}H_{30}N_{12}O_2$ ligand and a nitromethane molecule of crystallization are located on general positions. Three independent BF_4^- counterions are also present, all of which are rotationally disordered about 2-fold axes. A total of six restraints were used in modeling the anion disorder. Crystal data and refinement results for **1**−**3** are presented in Table 1, and ORTEP diagrams of the asymmetric unit for each (Figures S2−S4) are in the Supporting Information.

Results

Synthesis of Complexes. The reactions between silver tetrafluoroborate and ligands **L1**, **L2**, and **L3** yield three new coordination polymers as shown in the equations. All

(17) *SAINT+ Version 6.02a*; Bruker Analytical X-ray Systems, Inc.: Madison, WI, 1998.

(18) Sheldrick, G. M. *SHELXTL Version 5.1*; Bruker Analytical X-ray Systems, Inc.: Madison, WI, 1997.

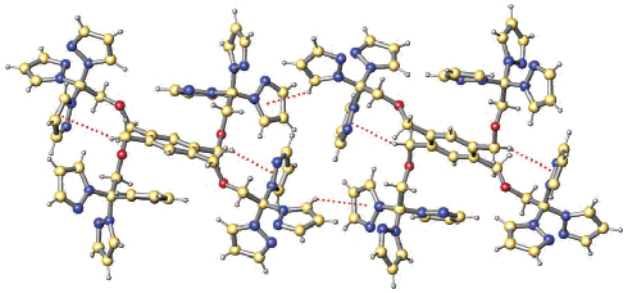

Figure 1. Structure of **L1** and its association in chains supported by intramolecular and intermolecular C−H···π interactions: carbon, yellow; nitrogen, blue; oxygen, red; hydrogen, gray. C−H···π interactions are shown as red dotted lines.

compounds are white powders that precipitated out from the reaction mixture and are air stable, showing only slight decomposition under daylight after several weeks. They are soluble in acetone, acetonitrile, and nitromethane but insoluble in halogenated solvents, water, or alcohols.

$$n\{C_6H_2[CH_2OCH_2C(pz)_3]_4\} + 2nAgBF_4 \rightarrow \{C_6H_2[CH_2OCH_2C(pz)_3]_4(AgBF_4)_2\}_n$$
1

$$n\{o\text{-}C_6H_4[CH_2OCH_2C(pz)_3]_2\} + nAgBF_4 \rightarrow \{o\text{-}C_6H_4[CH_2OCH_2C(pz)_3]_2(AgBF_4)\}_n$$
2

$$n\{m\text{-}C_6H_4[CH_2OCH_2C(pz)_3]_2\} + 2nAgBF_4 \rightarrow \{m\text{-}C_6H_4\{CH_2OCH_2C(pz)_3]_2(AgBF_4)_2\}_n$$
3

The ^{1}H NMR spectra of the solids **1**−**3** in CD_3CN show that the acetonitrile completely replaces the ligand; the spectrum of the compound in CD_3CN is the same as the free ligand in this solvent. However, ^{1}H NMR spectra of the compounds in deuterated acetone are clearly different from the free ligand, showing the coordination of the ligand to the silver(I) in this solution. Although the X-ray structure shows that in the solid state the pyrazolyl rings are nonequivalent (vide infra), the NMR spectra of the coordination polymers of silver show equivalent rings, presumably because of fast exchange of the ligands and metals on the NMR time scale.

X-ray Structures of Ligands. The structure of the tetratopic ligand 1,2,4,5-$C_6H_2[CH_2OCH_2C(pz)_3]_4$ (**L1**; see Figure S1 and Tables S1 and S2 in the Supporting Information for details), Figure 1, consists of discrete molecules, and within each tris(pyrazolyl)methane unit the orientation of the three pyrazolyl rings is a propeller arrangement. The adjacent arms of the ligand are oriented above and below the arene ring plane, with one arm twisted away from the other. This orientation is sustained by an intramolecular C−H···π interaction between a methylene hydrogen atom next to the arene ring on the arm that is twisted away and a pyrazolyl ring on the adjacent arm. The hydrogen atom is oriented over the pyrazolyl ring at a distance of 2.94 Å and the corresponding carbon atom at a distance of 3.67 Å, the value of the corresponding C−H···π angle being 132°. These values are typical for C−H···π interactions.[9] The molecule

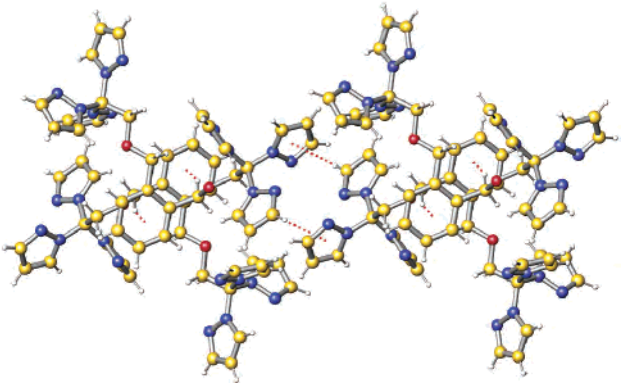

Figure 2. Formation of dimers and chains in **L2** by the means of C−H···π interactions pictured as red dotted lines.

is centrosymmetric, orienting the 1,4 and 2,5 pairs of tris(pyrazolyl)methane units on opposite sides of the arene ring. Intermolecular C−H···π interactions exist between a CH group located on a pyrazolyl ring and the π cloud from another pyrazolyl ring on a second molecule, shown as red dotted lines in Figure 1. The C(51)−H(51)···π contact is 2.97 Å (with C−centroid distance of 3.60 Å) with the corresponding angle of 126°. Two of these interactions associate adjacent **L1** ligands forming chains that run approximately along the *a* axis in the [110] plane.

The metrical parameters for the individual molecules of **L2** were described elsewhere,[16a] but for comparative purposes with **L1** additional information is shown in Figure 2. A double C−H···π interaction between two molecules, where hydrogen atoms from a methylene group next to a central arene ring orient above the centroid of the other central arene ring, indicated by the red dotted lines, organizes **L2** into dimers. The C−H···centroid distances are 2.70 Å (with C−centroid distances of 3.49 Å), with the corresponding angles of 138°. These dimers form chains in the [110] plane and bisect the angle formed by *a* and *b* axes via a second pair of C−H···π interactions between adjacent dimer units, the distances being of 2.96 and 3.88 Å respectively, with the corresponding C−H···centroid angles of 171° (red dotted lines). These associations show that **L2** can be considered as half of **L1** not only with respect to composition and position of sidearms but also with respect to the structures in the solid state. The first type of C−H···π interaction in **L2** connects two ortho ligands into a 1,2,4,5 dimeric unit that resembles the four arms ligand **L1**. The second C−H···π interaction for this dimer, $(\mathbf{L2})_2$, associates it into the same basic type of chains observed for **L1**.

X-ray Structures of Silver(I) complexes. Selected bond lengths and angles are listed in Table 2. The asymmetric unit of **1** contains one Ag atom, half a ligand, one BF_4^- counterion, and two acetonitrile molecules of crystallization. As can be seen in Figure 3, each silver atom is κ^2-bonded to two tris(pyrazolyl)methane units from different ligands, with each unit having one pyrazolyl ring that is not coordinated to a silver. The silver is in a distorted tetrahedral geometry, with the restraints imposed by the "bite" angle of the tris(pyrazolyl)methane unit lowering the angles

Table 2. Selected Bonds (Å) and Angles (deg) for **1**−**3**

	Compound 1		
Ag−N(11)	2.403(2)	N(11)−Ag−N(21)	80.60(8)
Ag−N(21)	2.274(2)	N(11)−Ag−N(51)	99.03(7)
Ag−N(51)	2.322(2)	N(11)−Ag−N(61)	138.74(9)
Ag−N(61)	2.315(2)	N(21)−Ag−N(51)	144.78(10)
		N(21)−Ag−N(61)	120.33(9)
		N(51)−Ag−N(61)	83.03(8)
	Compound 2		
Ag−N(11)	2.283(2)	N(11)−Ag−N(21)	83.12(8)
Ag−N(21)	2.341(2)	N(11)−Ag−N(51)	142.48(8)
Ag−N(41)	2.353(2)	N(11)−Ag−N(41)	124.05(8)
Ag−N(51)	2.271(2)	N(21)−Ag−N(41)	99.36(8)
		N(21)−Ag−N(51)	123.53(9)
		N(41)−Ag−N(51)	80.76(8)
	Compound 3		
Ag(1)−N(11)′	2.361(7)	N(11)′−Ag(1)−N(11)	103.2(3)
Ag(1)−N(11)	2.361(7)	N(11)′−Ag(1)−N(21)	141.2(2)
Ag(1)−N(21)	2.372(7)	N(11)−Ag(1)−N(21)	76.6(2)
Ag(1)−N(21)′	2.372(7)	N(11)′−Ag(1)−N(21)′	176.6(2)
Ag(2)−N(31)′	2.262(7)	N(11)−Ag(1)−N(21)′	141.2(2)
Ag(2)−N(41)	2.323(7)	N(21)−Ag(1)−N(21)′	127.7(4)
Ag(2)−N(51)	2.329(8)	N(31)′−Ag(2)−N(41)	155.1(2)
Ag(3)−N(61)	2.133(7)	N(31)′−Ag(2)−N(51)	112.1(2)
Ag(3)−N(61)′	2.133(7)	N(41)−Ag(2)−N(51)	81.2(2)
		N(61)−Ag(3)−N(61)′	180.0(2)

N(11)−Ag−N(21) and N(51)−Ag−N(61) to 80.60(8) and 83.02(8)°, respectively (Table 2).

The overall structure is a polymer made up of rings formed by two ligands bonding tris(pyrazolyl)methane groups from nonadjacent positions on the arene rings to the same two silver atoms, Figure 4. The arene groups link these 32-atom macrocycles into polymer chains. The holes formed by the rings are partially occupied by two of the pyrazolyl rings that are not coordinated to the silver. The orientation of these rings is supported by C−H···π interactions between the pyrazolyl rings occupying the holes and methylene hydrogen

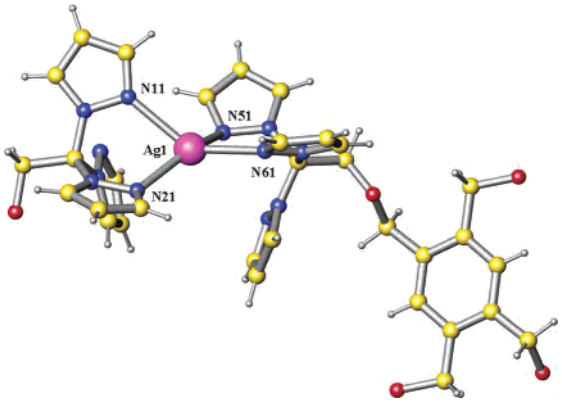

Figure 3. Coordination environment around the silver(I) atom in **1**.

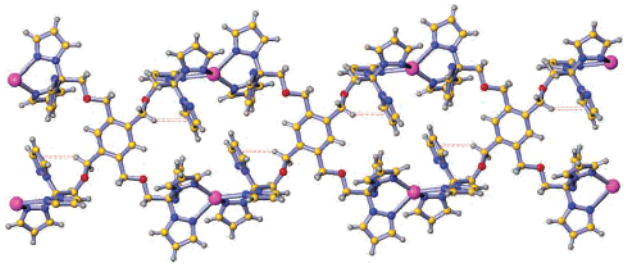

Figure 4. 1-D covalent network of **1**: carbon, yellow; nitrogen, blue; oxygen, red; hydrogen, gray; silver, purple. C−H···π interactions are shown as red dotted lines.

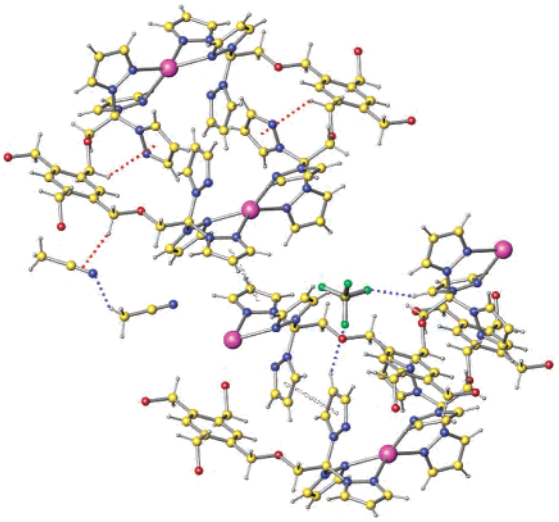

Figure 5. All noncovalent interactions in **1**, including the intrastrand C−H···π interaction of the noncoordinated pyrazolyl ring.

atoms next to the arene ring, with a H−centroid distance of 2.97 Å and with the corresponding C−centroid distance of 3.65 Å. These values, again, are typical for C−H···π interactions.[9]

There are two types of forces that organize the polymer strands into a supramolecular structure. As shown in Figure 5 as blue dotted lines, each BF_4^- makes two C−H···F weak hydrogen bonds. The C−H···F interactions, made between adjacent strands, are 2.40 and 2.48 Å, respectively, with the corresponding angles of 156 and 151°. While not strong interactions (the sum of van der Waals radii of fluorine and hydrogen atoms being 2.54 Å),[19] the bonds are close to linear. As stated for other types of weak interactions (e.g. weak C−H···O hydrogen bonds), bonds that are close to linear indicate a substantial interaction between the F and H atoms, even in cases where the distances are close to the sum of van der Waals radii.[20] As also shown in Figure 5, there are two π−π stacking interactions between strands, shown with black double dotted lines. The first interaction involves noncoordinated pyrazolyl rings that are oriented away from the polymeric strands and is between the same strands as those involved in the weak C−H···F hydrogen bond. The second involves two pyrazolyl rings coordinated to silver atoms and organizes strands oriented in the opposite diagonal direction to those joined by the first bonding interactions. In both cases the two pairs of pyrazolyl rings are displaced with centroid−centroid distances of 4.06 and 4.11 Å, respectively, and the rings are parallel with a perpendicular distance between the rings of 3.55 Å in the first case and 3.45 Å in the second case. This slippage of aromatic rings involved in π−π interactions is observed frequently, and 3.60 and 3.48 Å are short distances for this type of interaction.[8,21] In this configuration, an important contribution to the

(19) (a) Bondi, A. *J. Phys. Chem.* **1964**, *68*, 441. (b) Rowland, R. S., Taylor, R. *J. Phys. Chem.* **1996**, *100*, 738.
(20) (a) Steiner, T.; Desiraju, G. R. *Chem. Commun*. **1998**, 891. (b) Steiner, T.; Lutz, B.; van der Maas, J.; Schreurs, A. M. M.; Kroon, J.; Tamm M. *Chem. Commun*. **1998**, 171.
(21) (a) Wu, H.-P.; Janiak, C.; Rheinwald, G.; Lang, H. *J. Chem. Soc., Dalton Trans*. **1999**, 183.

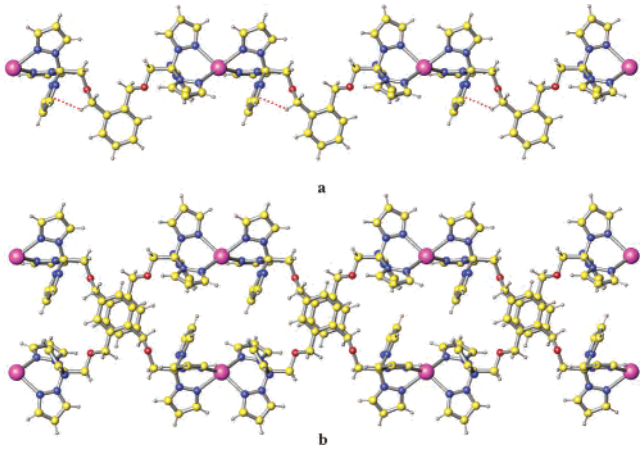

Figure 6. (a) One polymeric chain of **2**. Every second nonbonded pyrazolyl ring makes a C−H···π interaction with a CH_2 group. (b) Two strands of **2**, organized in polymeric dimers through a $\pi-\pi$ stacking interaction between the central arene rings.

attractive forces arises from a pronounced $\pi-\sigma$ attraction interaction of a C−H σ bond with the adjacent aromatic π cloud.[8]

The distance between two silver atoms in the 32-atom metallomacrocycles is 9.31 Å and between two equivalent silver atoms from adjacent macrocycles in the polymer chain is 14.93 Å. The corresponding Ag···Ag···Ag angles are 87 and 93°, respectively. Thus, as best seen in Figure 4, the silver atoms within the chain form an almost perfect series of rectangles. The closest distance between two silvers atoms from two chains involved in $\pi-\pi$ stacking is 6.93 Å.

Compound **1** also has two acetonitrile molecules of solvation (not bonded to silver) located in different positions, one being in the "$\pi-\pi$ stacking region" and another lying above the central arene ring, Figure 5. There is a C−H···N hydrogen bond (blue dotted line in Figure 5) between the acetonitrile molecules, with a H···N distance of 2.54 Å (C−N distance of 3.44 Å) and a corresponding C−H···N angle of 156°. Also organizing the solvent molecules in the crystal is an interaction of the triple bond of one of the acetonitrile molecules with a hydrogen atom located on a methylene group next to the central arene ring (red dotted line), with a C(3)−H(3b)···π distance of 2.90 Å (C···π distance of 3.62 Å) with the corresponding angle of 132°.

Compound **2** has an environment around the silver atom similar to that of **1**. As can be seen in Figure 6a, two pyrazolyl rings from two different ligands chelate the silver atoms in a distorted tetrahedral arrangement that is, again, strongly influenced by the "bite" angle of the tris(pyrazolyl)-methane unit. The N(11)−Ag−N(21) and N(41)−Ag−N(51) angles are 83.12(8) and 80.76(8)°, respectively, very close to the corresponding angles in **1** (Table 2). Each bitopic ligand bonds two silver atom in this $\kappa^2-\kappa^2$ fashion forming a polymer chain that runs along the *b* axis of the unit cell. There are also noncoordinated pyrazolyl rings, one from each unit, oriented away from the strand. The central arene rings are situated on the same side of the polymeric chain, in contrast with the cadmium analogue[16a] where the central arene ring was found at alternate sides along the strand. Half of the noncoordinated pyrazolyl rings are oriented toward a

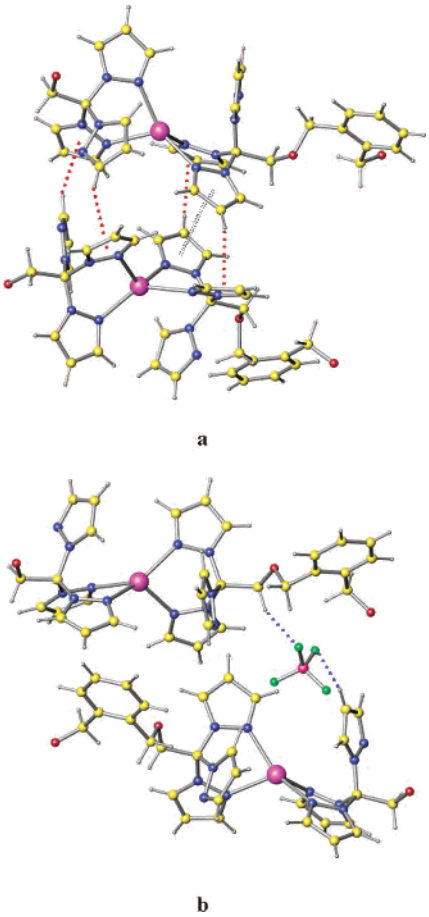

Figure 7. All noncovalent interactions in **2**: (a) $\pi-\pi$ stacking and C−H···π interactions between two polymeric strands; (b) weak C−H···F interactions between two strands.

methylene group adjacent to the central arene ring. This orientation is supported by a C−H···π interaction (pictured as red dotted line in Figure 6a) between this pyrazolyl ring and one hydrogen atom from the methylene group, with a short H(78b)−centroid distance of 2.60 Å and with the corresponding C(78)−centroid distance of 3.29 Å.[9]

The strands are organized into dimers, shown in Figure 6b, through face-to-face $\pi-\pi$ stacking between the central arene rings, with a perpendicular distance between planes of 3.57 Å. The presence of the two adjacent electron-withdrawing sidearms induces opposite polarization in each pair of central arene rings, making the stacking more effective. Also, it leads to a parallel displacement of the rings; therefore, the centroid−centroid distance is 3.99 Å. The distance between the silver atoms in the strand is 14.94 and 8.73 Å within a dimer. The corresponding Ag···Ag···Ag angles within the dimer are both 90°. The $\pi-\pi$ stacking interactions between the central arene rings cause **2** to form dimeric strands that appear very similar to those of **1**, Figure 4.

These dimeric chains are organized further into a 3-D architecture by three additional types of noncovalent interactions. Figure 7 shows the additional noncovalent interactions that influence the extended structure of **2**. First, the dimeric strands are arranged in sheets via a face-to-face $\pi-\pi$ stacking between two pyrazolyl rings coordinated to silver,

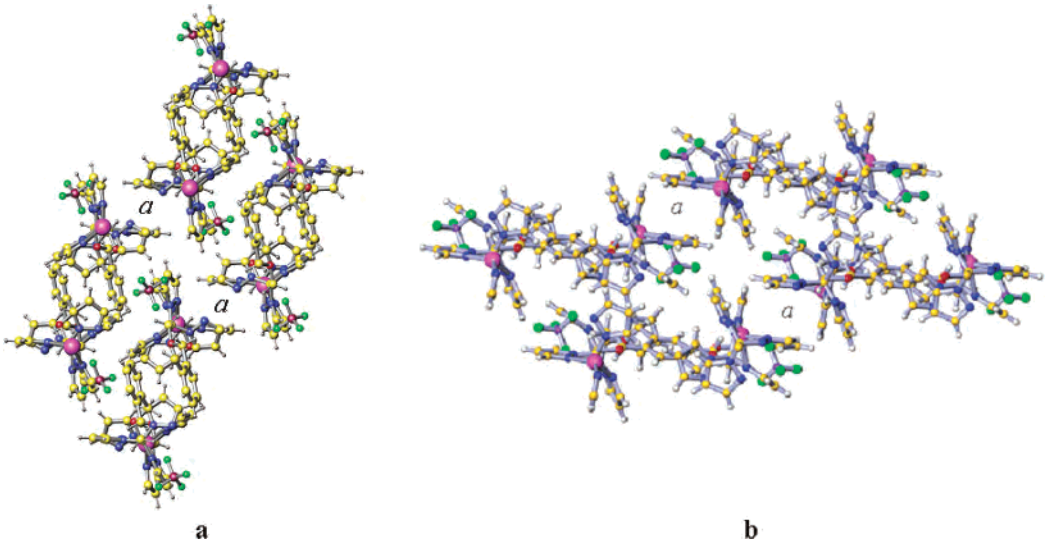

Figure 8. Comparison between the extended structures of **1** and **2**: (a) crystal packing of four dimeric strands of **2**; (b) crystal packing of four strands of **1**. *a* indicates the $\pi-\pi$ stacking region, organizing the dimers/strands into sheets; the C−H···F hydrogen bonds are oriented in the opposite diagonal direction to those involved in $\pi-\pi$ stacking.

black double dotted lines in Figure 7a. The shortest distance, C(51)−C(51′), is 3.42 Å and the longest, N(51)−C(53′) is 3.72 Å, with a centroid−centroid distance of 3.55 Å, showing a strong interaction between dimers. This arrangement is also supported by several C−H···π interactions, shown in Figure 7a as red dotted lines. First, the pyrazolyl rings involved in $\pi-\pi$ stacking have their C(52)−H(52) bond directed toward another pyrazolyl ring bonded to silver, the H···centroid distances being 2.75 Å (with a C−centroid distance of 3.61 Å) with a corresponding angle of 151°. Second, the uncoordinated pyrazolyl ring not involved in the intrachain C−H···π interaction mentioned above is pointed toward a coordinated pyrazolyl ring from an adjacent strand, the H(33)···centroid distances being 2.86 Å (with a C−centroid distance of 3.74 Å) with a corresponding angle of 154°. These sheets are arranged in a 3-D architecture by C−H···F weak hydrogen bonds. As shown in Figure 7b (blue dotted lines), each BF_4^- ion makes two short interactions between a methylene group and a pyrazolyl ring situated on adjacent strands, with distances of 2.40 and 2.37 Å, respectively, with the corresponding angles of 138 and 165°.

Figure 8a depicts the packing of four dimeric strands of **2**, together with the counterions, viewed down the polymer chain of the strands; Figure 8b provides an analogous view for compound **1**. In these orientations, the $\pi-\pi$ stacking interactions and C−H···π interactions between dimer/polymeric units are arranged vertically (indicated by *a* in the Figure). The C−H···F interactions are between the strands oriented in the opposite diagonal direction than those involved in $\pi-\pi$ stacking. Although the orientation of the elongated axis of the dimer/polymeric units is different, the supramolecular organization is surprisingly similar.

In contrast to compounds **1** and **2**, where the ratio of tris(pyrazolyl)methane units to silver is 2:1, the ratio expected for a simple coordination polymer, this ratio is 1:1 in *m*-$C_6H_4[CH_2OCH_2C(pz)_3]_2(AgBF_4)_2$, **3**. Compound **3** contains three different types of silvers, tetrahedral Ag(1), trigonal Ag(2), and linear Ag(3), in a ratio of 1:2:1, and all

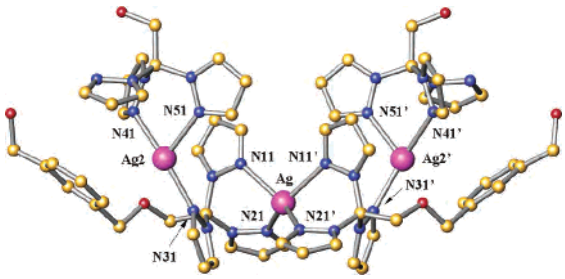

Figure 9. Coordination environment of Ag(1) and Ag(2). Only essential atoms are shown.

of the pyrazolyl rings are coordinated to one of the silvers. Figure 9 shows the environment of Ag(1) and Ag(2). As in the structures of **1** and **2**, the environment around Ag(1) is a distorted tetrahedron, with two pyrazolyl rings from two tris(pyrazolyl)methane units located in different ligands bonded in a $\kappa^2-\kappa^2$ fashion. The bond lengths and angles (see Table 2) are close to the values observed for **1** and **2**, as expected. The third pyrazolyl ring from each of the tris(pyrazolyl)methane units bonded to Ag(1) is κ^1-bonded to a second silver atom, Ag(2). The coordination sphere of each Ag(2) is completed by κ^2-bonding by two pyrazolyl rings from a tris(pyrazolyl)methane unit located in a different ligand. The environment about Ag(2) is a flattened trigonal pyramid (sum of the N(41)−Ag(2)−N(51) bond angles = 348.42°), with a significant distortion caused by the restricted angle (81.2(2)°) of the κ^2-bonded ligand.

The coordination around the third silver atom (Ag(3)) is pictured in the center of Figure 10. The remaining pyrazolyl rings from two tris(pyrazolyl)methane units κ^2-bonded to Ag(2), located in different ligands, are coordinated to Ag(3), with the N(61)−Ag(3) distance being 2.133(7) Å and the corresponding angle 180°. Furthermore, two pyrazolyl rings coordinated to Ag(2) are oriented toward Ag(3), each centroid−Ag(3) distance being 3.15 Å with the corresponding angle of 180°. Several studies on arene−silver interactions, including a statistical analysis based on the existing

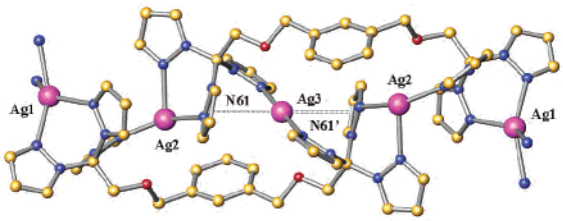

Figure 10. Coordination around the Ag(3) atom, with two ligands closing a macrocycle. Hydrogen atoms not shown.

structures in the Cambridge Structural Database,[22] reported a range of Ag−centroid distances of 2.89−3.37 Å.

Overall from left to right in Figure 10, the polymeric chains of **3** are formed in the following manner: one tris(pyrazolyl)methane unit from a bitopic ligand is κ^2-bonded to Ag(1) and κ^1-bonded to Ag(2). The other tris(pyrazolyl)methane unit in this ligand is κ^2-bonded to Ag(2′) and κ^1-bonded to Ag(3). A tris(pyrazolyl)methane unit in a second ligand bonds κ^2 to the Ag(2) that is κ^1-bonded by the first ligand and κ^1 to Ag(3), that is also κ^1-bonded by the first ligand. The second tris(pyrazolyl)methane unit in this second ligand bonds κ^1 to Ag(2′), which is κ^2-bonded by the first ligand and bonds κ^2 to Ag(1′) to continue the polymer chain. This arrangement generates the following sequence of silver atoms along the polymer strand: Ag(1)−Ag(2)−Ag(3)−Ag(2)−Ag(1). There are twice as many Ag(2) as Ag(1) or Ag(3). The structure of **3** can also be regarded as an infinite chain of 32-atom metallomacrocycles, containing two Ag(2) and two ligands. The Ag(3) "short circuits" the large metallomacrocycles into two 22-atom smaller metallomacrocycles, and the large metallomacrocycles are bridged into polymer chains by Ag(1).

As pictured in Figure 11, the overall shape of the coordination polymer is sinusoidal with Ag(1) at the maxima; the "wavelength"—measured between every other Ag(1)—is 33.17 Å. The same distance is found between every other Ag(3) and between every fifth Ag(2). The distance between any consecutive Ag(1)···Ag(2) is 4.90 Å and between any consecutive Ag(2)···Ag(3) is 5.20 Å. Supporting this structure are C−H···π interactions between a hydrogen from a methylene group next to the central arene ring and the π cloud from a pyrazolyl ring that is κ^1-bonded to Ag(2). The H···centroid and C−centroid distances are 2.87 and 3.56 Å respectively, with the corresponding angle of 128°.

An important structural feature is that the tris(pyrazolyl)methane units of each ligand are oriented on the same side of the central arene ring, placing these rings, in an alternate fashion, on the outside of the strands. Face-to-face, $\pi-\pi$ stacking of these central arene rings, with several short C−C distances at 3.58 Å, organize the polymeric strands into a 2-D array, Figure 12. The presence of the two electron-withdrawing sidearms in the 1- and 3-positions induces a polarization in the arene ring, making the stacking more effective, and also leads to a parallel displacement of the rings (centroid−centroid = 4.06 Å). The $\pi-\pi$ stacking is in the [010] direction, the distances between equivalent silver atoms located in adjacent strands being equal with the value of the *b* axis, 13.1641(8) Å.

The 2-D sheets formed by the $\pi-\pi$ stacking are parallel, with the counterions located between the sheets and located near the maxima points of the sinus, with the $\pi-\pi$ stacking organizing the vertical pairs, Figure 13. The BF_4^- counterions presumably organize these sheets into a 3-D array, but since the anions were found to be disordered, detailed information on individual interactions is not available.

Infrared Studies. Solid-state structures of the ligands and all three compounds reported here revealed the presence of three types of noncovalent interactions between the ligand molecules or the polymeric strands of **1**−**3**, manifested by close contacts between several atoms. These types of interactions can also be studied by IR spectroscopy. Classic hydrogen bonding (X−H···Y)[6,7] involves two electron-withdrawing atoms, one having a hydrogen atom attached and the second carrying lone electron pairs, and there must be a significant charge transfer from the proton acceptor (Y) to the proton donor (X−H). The formation of a hydrogen bond is followed by a lengthening of the donor X−H bond with a concomitant red shift in the ν(X−H) frequency. Many structural data and theoretical studies[9] have extended the concept of hydrogen bonding to the X−H···π (X = C, N, O) type interaction. In contrast to the classical hydrogen bond, frequently the formation of such a hydrogen bond is followed by a shortening of the donor X−H bond with a concomitant blue shift in the X−H frequency.[23] This interaction, first called "anti-H bond" and then, more accurately, improper H-bond,[23c] has the same features as the classic H-bond; there is a charge transfer from the proton acceptor (i.e. the π cloud originated from an aromatic ring) followed by a stabilization of the "complex", due to the dispersion and electrostatic quadrupole−quadrupole interactions.[23]

Since the solid-state structures indicate that all the compounds reported here present both classic and improper hydrogen bonds, IR spectra of the compounds were used to confirm the presence of both of these noncovalent interactions. The bands in the vibrational spectra of the compounds have been partially assigned. The assignments are listed in Table 3 and were made by comparisons to literature data[24] and the spectrum of the parent $HC(pz)_3$ ligand. There are two regions of interest, 4000−2800 and 1750−400 cm^{-1}. The IR spectra were recorded in solution ($CDCl_3$) only for the free ligands, due to the insolubility of the metal

(22) (a) Mascal, M.; Kerdelhue, J. L.; Blake, A. J.; Cooke, P. A. *Angew. Chem., Int. Ed.* **1999**, *39*, 1968. (b) Mascal, M.; Kerdelhue, J. L.; Blake, A. J.; Cooke, P. A.; Mortimer, R. J.; Teat, S. J. *Eur. J. Inorg. Chem.* **2000**, 485.

(23) (a) Hobza, P. *Phys. Chem. Chem. Phys.* **2001**, *3*, 2555. (b) Reimann, B.; Buchhold, K.; Vaupel, S.; Brutschy, B.; Havlas, Z.; Spirko, V.; Hobza, P. *J. Phys. Chem. A* **2001**, *105*, 5560. (c) Hobza, P.; Havlas, Z. *Chem. Rev.* **2000**, *100*, 4253. (d) Muller-Dethlefs, K.; Hobza, P. *Chem. Rev.* **2000**, *100*, 143. (e) Cubero, E.; Orozco, M.; Hobza, P.; Luque, F. J. *J. Phys. Chem. A* **1999**, *103*, 6394. (f) Hobza, P.; Spirko, V.; Havlas, Z.; Buchhold, K.; Reimann, B.; Barth, H. D.; Brutschy, B. *Chem. Phys. Lett.* **1999**, *299*, 180. (g) Hobza, P.; Spirko, V.; Selzle, H. L.; Schlag, E. W. *J. Phys. Chem. A* **1998**, *102*, 2501.

(24) (a) Kuznetsov, M. L.; Dementiev, A. I.; Krasnoshchoikov, S. V. *J. Mol. Struct. (THEOCHEM)* **1998**, *453*, 17. (b) Diaz, G. F.; Campos, M. V.; Klahn, A. H. O. *Vib. Spectrosc.* **1995**, *9*, 257.

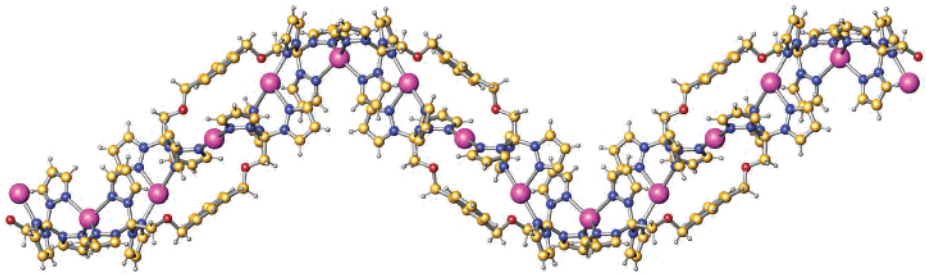

Figure 11. Structure of **3**. In this orientation Ag(1) is positioned at the maxima of the sinusoidal chain.

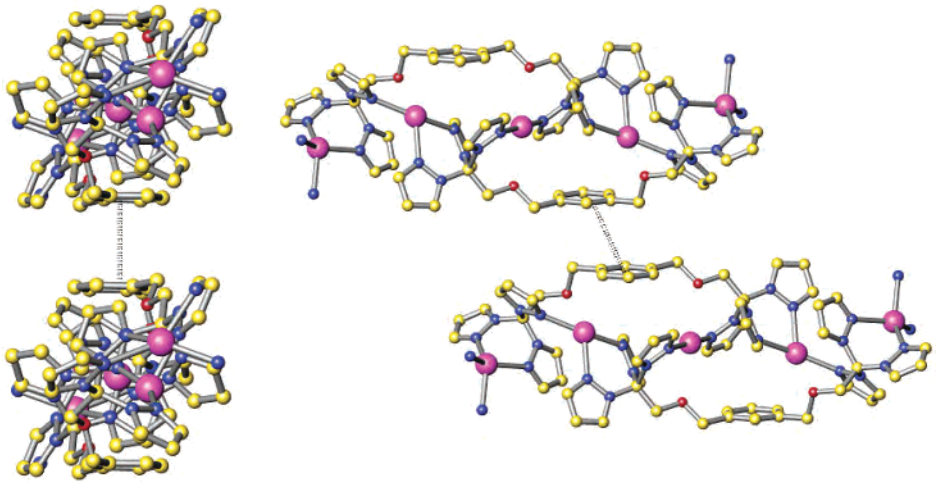

Figure 12. $\pi-\pi$ stacking between two central arene rings in **3**: left, view of $\pi-\pi$ sacking region down to the polymer strands; right, view nearly perpendicular to the macrocyclic rings formed by two ligands.

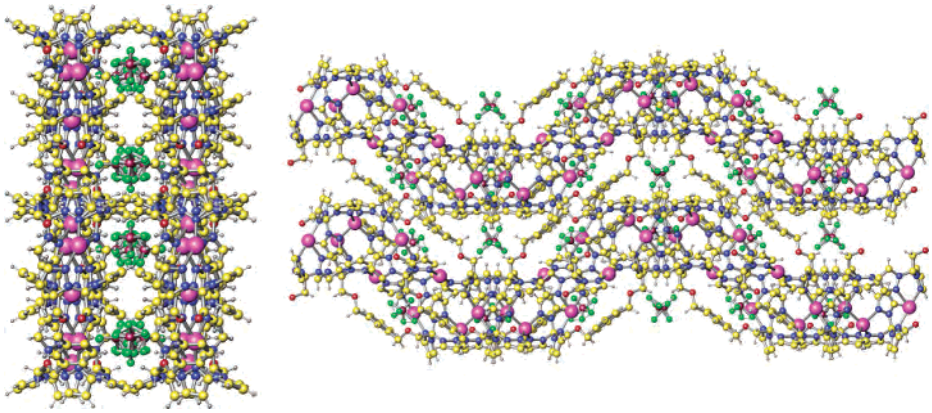

Figure 13. Crystal packing of **3**, showing two sets of two stacked strands together with the disordered BF_4^- counterions: left, view along sheets; right, view perpendicular to sheets.

complexes in solvents other than acetone, acetonitrile, and nitrometane—solvents presenting strong vibrations in the regions of interest. The IR spectra in the solid state were recorded using crystals from the same batch used in crystal structure determinations for both ligands and complexes (**L3** has not been crystallized). Also, for comparison purposes, we recorded the spectra of noncrystalline samples of the three complexes, using the white powders obtained from the reaction mixtures.

As can be seen in Table 3, in solution, all ligands show three vibrations in the first region, at 3155, 2985, and 2902 cm^{-1}, corresponding to the C−H vibrations originated from the pyrazolyl ring, central arene ring, and methylene groups, respectively. In the solid state, multiple bands appear in these regions for all compounds studied. Although some bands appear at higher wavenumbers for all six compounds (see Table 3), it is difficult to assume that this is the blue-shift effect of the improper hydrogen bond, although we cannot rule out this possibility. More studies on additional compounds will be needed to definitively settle this issue. In addition, compound **1** has two strong vibrations at 3639 and 3557 cm^{-1}, due to the hydrogen bonding of the acetonitrile molecules of solvation, also observed in the crystallographic studies. Free acetonitrile has two vibrations at 3653 cm^{-1} and 3618 cm^{-1} that correspond to C−H···N hydrogen bonds in solution, and the red shifts of the crystalline samples of

Table 3. Infrared Data

L1		L2		L3					
soln	cryst	soln	cryst	soln	oil	**1** (cryst)	**2** (cryst)	**3** (cryst)	assgnts
						3639 s			$\nu(CH_3)$ (CH_3CN)
						3630 sh			
						3557 s			
3155 s	3165 wm	3155 m	3155 ms	3155 m	3157 m	3158 sh	3159 sh	3160 s	ν(CH) (pyrazole)
	3152 m		3123 s	3114 w	3129 s	3148 s	3150 s	3147 s	
	3130 s				3108 m	3134 s			
	3118 m								
	3107 sh								
2985 s	2956 m	2985 m	3068 m	2984 m	2948 m	3024 w	3070 w	3020 w	ν(CH) (central arene ring)
	2937 s		3043 w				3064 w		
	2927 s		3014 w				3031 wm		
2902 m	2892 w	2901 m	2940 ms	2902 m	2929 m	2977 w	2971 w	2928 wm	$\nu(CH_2)$ (sidearms)
	2886 w		2927 m		2887 m	2940 w	2958 w	2885 m	
	2869 w		2901 m		2866 w	2928 wm	2926 m		
			2883 m			2900 w	2900 m		
1646 m	1616 br	1643 m	1610 br	1646 m	1631 m	1630 m	1609 br	1618 br	arene and pz ring str
1602 w		1602 w		1602 w	1610 w				
1560 m	1540 w	1561 w	1541 w	1560 m	1555 w	1560 w	1560 w	1561 s	arene and pz ring str
1517 ms	1517 s	1518 m	1517 m	1518 m	1515 ms	1518 ms	1522 s	1523 m	
1471 s	1480 m	1471 s	1482 m	1471 s	1471 m	1472 w	1481 w	1473 w	
1426 m	1459	1426 m	1454	1425 m	1451	1458	1465	1458	$\delta(CH_2)$ scissor
	1424		1421		1425	1438	1431	1428	
						1422			
1336 ms	1329 s	1336 s	1333 s	1336 s	1331 s	1337 s	1343 s	1335 s	pz ring str
			1322 s			1327 s	1327 s		
1216 m	1227 m	1216 m	1222 m	1216 m	1237 sh	1225 m	1218 ms	1229 m	$\delta(C(pz)_3)$
1202 ms	1202 s	1202 ms	1201 s	1202 s	1203 s	1211 ms	1211 ms	1212 ms	
						1200 ms	1205 ms	1204 ms	
1094	1092 s	1094 s	1093 s	1094 s	1092 s	1106−1048 br	1104−1032 br	1108−1036 br	see text
	1070−1023		1068−1024		1062−1037				
	948 s		949 s		949 s	957 ms	958 ms	967 w	substituted aromatic ring
						951 ms	947 ms	952 ms	out-of-plane deformations
						521 m	521 ms	521 ms	$\nu_4(F_2)$ (BF_4^-)

14 and 61 cm^{-1}, respectively, are an indication of stronger C−H···N hydrogen bond between the acetonitrile molecules in the solid.

The $\delta(CH_2)$ scissor vibrations prove useful for observing C−H···π interactions because the bands were well separated from others in the compounds. The presence of C−H···π interactions should lead to the observation of higher frequency vibrations.[25] In solution, the free ligands show one band at 1426 cm^{-1}. In the crystalline state of the ligands and the metal complexes we observe a band in this same region and, in addition, a second band ca. 30 cm^{-1} higher than the first; see Table 3. Crystallographic studies showed that some of the methylene groups are involved in C−H···π interactions and some are not, leading to the expectation of two separate vibrations, with the bands for the CH_2 groups involved in C−H···π interactions at higher frequencies than the for the CH_2 groups not involved in C−H···π interactions. Although the infrared data do support the C−H···π interactions, the shifted values are close and cannot be used to judge the relative *strength* of the interactions. For **1**, the only complex where two methylene groups are involved in two different C−H···π interactions in the crystalline state, two different $\delta(CH_2)$ vibrations were found at 1458 and 1438 cm^{-1}, together with the free $\delta(CH_2)$ vibration at 1422 cm^{-1}.

The characteristic vibrations of the anion showed its involvement in weak C−H···F hydrogen bonds. The BF_4^- counterion of T_d symmetry presents four modes of vibration, all of them active in the Raman and only two in the IR. In the crystal, the symmetry of the anion is lowered; thus, the forbidden bands $\nu_1(A_1)$ and $\nu_2(E)$ can appear in the IR spectra of compounds. The strong $\nu_3(F_2)$ characteristic vibration (around 1070 cm^{-1} for the free BF_4^-)[25] was used by others to determine the behavior of BF_4^- in several compounds.[26] However, in the compounds reported here the free ligands present strong vibrations in the same region, at 1093 cm^{-1} for $\nu(CH_2-O-CH_2)$ and multiple bands in the interval 1068−1023 cm^{-1} for substituted aromatic ring. The overlap of these vibrations with the $\nu_3(F_2)$ vibration of the BF_4^- anion leads to the appearance of a very broad peak in the region of 1110−1030 cm^{-1} for all three compounds, making the assignments impossible. However, the $\nu_4(F_2)$ vibration of the BF_4^- anion can also be used in gaining information about the participation of the counterion in weak C−H···F hydrogen bonds. In compounds where the anion is not interacting (e.g. KBF_4), this vibration appears as a broad, weak peak around 533 cm^{-1},[25] while in our crystalline complexes this vibration was identified at 521 cm^{-1} as a sharp, strong peak (see Figure S5). This change in strength and the red shift of 12 cm^{-1} show that the fluorine atoms are involved in hydrogen bonds. It is important to note that in the IR spectra of amorphous powder samples of **1** and **2** (the precipitate obtained after the thf reaction and prior to

(25) Nakamoto, K. *Infrared and Raman Spectra of Inorganic and Coordination Compounds*, 3rd ed.; Wiley-VCH: New York, 1978.

(26) (a) Jesih, A. *J. Fluorine Chem.* **2000**, *103*, 25. (b) von Barner, J. H.; Andersen, K. B.; Berg, R. W. *J. Mol. Liq.* **1999**, *83*, 141. (c) Mu, S.; Kan, J. *Synth. Met.* **1998**, *98*, 51.

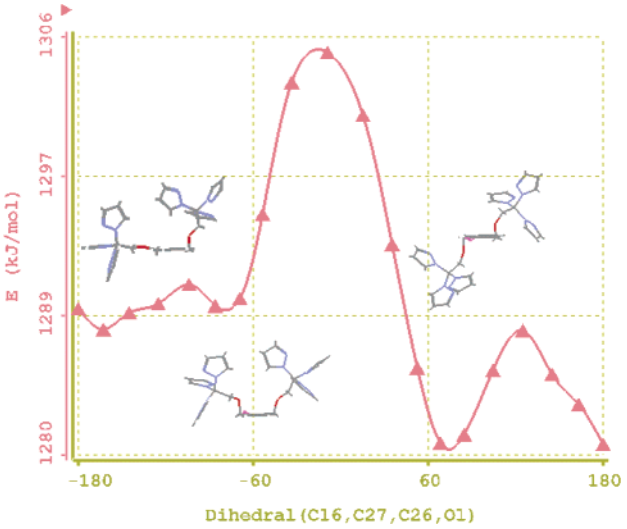

Figure 14. Classes of conformers for **L2**. From left to right they are noted as "in-plane_up", "up_up", and "up_down".

crystallization), the $\nu_4(F_2)$ vibration was identified as a small and broad peak at 529 cm^{-1}, close to the value for the noninteracting anion. These values, together with the intensity increase of the peak for the crystalline samples, show that in **1** and **2** the BF_4^- moiety is not involved in hydrogen bonding in the powder state but is in the crystalline state. Surprisingly, the ν_4 band in the powder sample of **3** appeared at 522 cm^{-1} as a sharp peak, presumably indicating that in this case there are some C−H···F interactions even in the powder obtained after the thf reaction.

Theoretical Studies. A conformational analysis on **L2** has been carried out using the Spartan 02 package.[27] Molecular orbital calculations at the PM3 semiempirical level reveal the existence of three classes of conformers (noted as up_up, up_down and in-plane_up with respect to the orientation of the sidearms) for this ligand. Figure 14 shows the variation of the enthalpy of formation (in gas phase) with the C16−C27−C26−O1 dihedral (defining the rotation of the pyrazolyl fragment around the arene−carbon bond). These data suggest that the most favored conformer is the up_down and it is separated by ca. 18−20 kJ/mol from the up_up and in-plane_up conformers. The lowest energy conformer in gas phase differs from the one observed in the solid state.[16a] The associations between the **L2** molecules in dimers via C−H···π interactions, as discussed above, prevents the up_down conformer and leads to the observed in-plane_up conformer. The C−H···π interactions overcomes the ca. 20 kJ/mol difference between the favored up_down class of conformers and the in-plane_up conformer found in solid state. In contrast, in the case of **L1** there is no *intermolecular* C−H···π interaction and the observed up_down orientation of 1,2- and 4,5-positions of the sidearms in the solid-state structure matches that predicted by theory. Furthermore, this up_down orientation found in the solid state of **L1** favors the *intramolecular* C−H···π interaction between a methylene hydrogen next to the central arene ring on one arm and a pyrazolyl ring on the adjacent arm (see Supporting Information, Figure S1, and also ref 16b).

(27) *Spartan '02*; Wavefunction, Inc.: Irvine, CA, 2002.

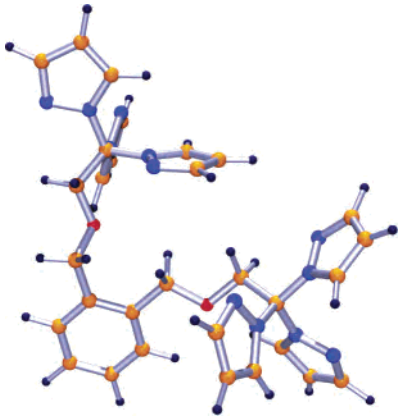

Figure 15. Optimum structure of the in-plane_up confomer of **L1** in the gas phase calculated at the DFT (B3LYP/6-31G*) level of theory.

A complete geometry optimization has been performed on the in-plane_up class observed in the solid-state structure at the DFT (B3LYP/6-31G*) level of theory.[28] The optimum structure is shown in Figure 15. One relevant feature of this conformation is the orientation of the CH_2-O-CH_2 moiety of one arm toward a pyrazolyl ring located on the adjacent arm. Interestingly, the H···pyrazolyl ring distances fall within the range of C−H···π contacts. Given this result, it is not surprising that we observe C−H···π interaction between the methylene and pyrazolyl groups in the solid-state structures.

Electrospray Ionization Mass Spectrometry Studies (ES-MS). ES-MS spectra for all three compounds were recorded in acetone and acetonitrile. For complexes **1** and **2**, the spectra are similar in both solvents. ES-MS of **1** in acetone shows two single-charged species, corresponding to $[(\mathbf{L1})Ag]^+$ at *m*/*z* 1121 and to $[(\mathbf{L1})Ag_2(BF_4)]^+$ at *m*/*z* 1405. A double-charged species was observed at *m*/*z* 659, corresponding to $[(\mathbf{L1})Ag_2]^{2+}$. In acetonitrile, the same three peaks were observed, although in acetone the most abundant species was the double charged peak at *m*/*z* 659, while in acetonitrile the most abundant peak was the single-charged species at *m*/*z* 1121 corresponding to $[(\mathbf{L1})Ag]^+$. For **2**, the ES-MS experiment in both acetone and acetonitrile revealed a peak at *m*/*z* 697, corresponding to the $[(\mathbf{L2})Ag]^+$ species, along with other peaks at lower values corresponding to silver−solvent adducts. For **3**, the ES-MS spectra were solvent dependent. In acetonitrile only one peak at *m*/*z* 697 was observed, corresponding to $[(\mathbf{L3})Ag]^+$ species. In acetone, although the most abundant peak also corresponded to $[(\mathbf{L3})Ag]^+$ species at *m*/*z* 697, a second peak was observed at *m*/*z* 893 corresponding to $[(\mathbf{L3})Ag_2(BF_4)]^+$ species.

Discussion

Given that the bitopic ligands **L2** and **L3** can each be considered half of the tetratopic ligand **L1**, comparisons of the supramolecular structures of the silver(I) coordination polymers formed by each provides an indication of the relative organizing power of the covalent and noncovalent interactions. The polymeric strand of **1** (Figure 4a) and the dimeric polymer unit formed by the association between two

(28) Becke, A. D. *J. Chem. Phys.* **1993**, *98*, 5648.

strands of **2** (Figure 6b) are very similar, not only with respect to the silver environment but in the overall arrangement of the organic ligands. In **1**, the polymer chain is formed by linking macrocyclic rings containing two four-coordinate silvers by the central arene ring. The same is true for **2**, except in this case the "rings" are joined by the $\pi-\pi$ stacked central arene rings of two polymer strands. This $\pi-\pi$ stacking in **2** essentially converts two of the bitopic ligands **L2** into an analogue of the tetratopic ligand **L1**. In both compounds, two uncoordinated pyrazolyl rings located in the center of the rings are involved in intrastrand C−H···π interactions. This interaction is stronger in **2** (2.60 Å) than in **1** (2.97 Å) because in the latter case the pyrazolyl ring involved in the interaction has steric contacts with other rings located across the macrocycle, whereas with **2** these interactions are removed because the pyrazolyl rings across the "ring" are in a different plane.

The two structures are also very similar with respect to Ag···Ag distances and angles. As expected, the distances between two equivalent silver atoms in a strand are almost equal, but surprisingly the Ag···Ag distance across a macrocycle in **1** and the analogous Ag···Ag distance within a dimer are almost equal. Also, the corresponding Ag···Ag···Ag angles are similar and near 90° in both **1** and **2**. The striking similarity between the structures of **1** and **2** in the organization of the strands (in the case of **1**) and dimeric strands (in the case of **2**) into a 3D network by means of $\pi-\pi$ stacking, C−H···π interactions, and weak hydrogen bonds causes other close silver atom distances to be similar in the two complexes. Figure 8 pictures four dimers (Figure 8a) and strands (Figure 8b) viewed down the polymer chain. The 3-D structures of both compounds are dominated by similar $\pi-\pi$ stacking interactions between strands or dimers, indicated by the *a*, and C−H···F interactions (each BF_4^- anion involved in two interactions in both compounds!) between the strands oriented in the opposite diagonal direction than those involved in $\pi-\pi$ stacking. A difference between the structures is that the elongated axis of the dimer strands in **2** are rotated 90° with respect to the strands in **1**, such that the central arene rings are oriented horizontally in **1** while in **2** they are oriented vertically. *In these structures,* **L2** *can be regarded as the half of* **L1** *and the noncovalent interactions overcome the geometrical differences between these two ligands leading to very similar supramolecular structures.*

Although **L3** can also be considered as half of **L1**, the structures and formulas of the silver complexes are different. For **1** and **2** the ratio of tris(pyrazolyl)methane units/silver is 2:1 and all silvers are four-coordinate with one noncoordinated pyrazolyl ring/tris(pyrazolyl)methane unit. For **3** the ratio is 1:1 and all pyrazolyl rings are bonded to one of the three different types of silvers, leading to a very different supramolecular structure. Clearly, the covalent forces that favor all of the pyrazolyl rings bonding to silver force a very different structure on **3** when compared to **1**. Interestingly, although the overall structure and formula are different, there is still a macrocycle present in the structure of **3** containing the same number of atoms, 32, as the macrocycle in **1** but with a different overall organization. The macrocycle is formed by the coordination of two ligands to two different types of silver atoms, Figure 10. One tris(pyrazolyl)methane unit from one sidearm of the ligand is coordinated in a κ^2 fashion to Ag(2). The other tris(pyrazolyl)methane unit from the second sidearm is κ^1 coordinated to the second Ag(2), thus closing the macrocycle, but is also κ^2 bonded to Ag(1) to form the polymer chain. The major difference is that two of the pyrazolyl rings that are noncoordinated in **1** are bonded to Ag(3), forming a connection across the larger, 32-member ring. In these structures, **L3** cannot be regarded as the half of **L1**.

These three structures show the *structurally adaptive* nature of this family of ligands. These semirigid ligands have the organizational features of containing multiple tris(pyrazolyl)methane units, each of which can show a variety of coordination modes, and contain functional groups that can enter into noncovalent forces such as weak hydrogen bonds, intermolecular and/or intramolecular $\pi-\pi$ stacking, and C−H···π interactions. The *ortho* orientation of the sidearms in **L1** and **L2** with a metal such as silver(I) that prefers low coordination numbers favors the formation of macrocycles, even at the expense of leaving potential donor atoms noncoordinated. For **L3**, all of the possible coordination sites in the ligands are bonded to silver(I), and these covalent interactions dominate the structure. Both the flexibility of the ligand sidearms and the organization features of the ligands contribute to the highly organized structures of these complexes.

Infrared studies have clearly been able to substantiate the C−H···F weak hydrogen bonding and C−H···π interactions identified in the solid-state structures. The $\nu_4(F_2)$ vibration of the BF_4^- anion was most useful in identifying participation of the counterion in weak C−H···F hydrogen bonds. Crystalline samples of all three complexes show a sharp, strong peak at 521 cm^{-1}, a peak that is weak in simple salts of the anion and in powder samples of **1** and **2**. Surprisingly, a sharp ν_4 band at 522 cm^{-1} was observed in the powder sample of **3**, indicating C−H···F interactions even in the powder state.

The $\delta(CH_2)$ scissor vibrations were most useful in studying the C−H···π interactions. In solution the free ligands show only one band at 1426 cm^{-1}, but in the solid state we observe a band in this same region and, in addition, a second band ca. 30 cm^{-1} higher than the first. These bands confirm C−H···π interactions observed in the crystallographic studies. The gas-phase calculations of the in-plane_up orientation of the **L2** conformation also show a C−H···π interaction of the CH_2-O-CH_2 moiety of one arm with a pyrazolyl ring located on the adjacent arm.

The ES-MS data collected from acetone or acetonitrile show the presence in solution of aggregated species related to those observed in solid state. All peaks correspond to one ligand and one or two silver ions with and without counterions. The similarity of ES-MS spectra of the compounds in acetone and acetonitrile is surprising because the ^1H NMR spectra of all compounds show that acetonitrile completely displaces the ligand whereas in deuterated acetone all

resonances are shifted from the free ligand, showing the coordination of the ligand to silver(I). This means that the same aggregates that exist in solution (acetone) are formed when a solvent (acetonitrile) that can displace the tris(pyrazolyl)methane ligand is removed in the electrospray process.

Conclusion

A combination of X-ray crystallography, IR spectroscopy, DFT calculations, and ES/MS studies has been used to investigate the solid-state and solution properties of silver(I) complexes formed from closely related semirigid, multitopic ligands, one of which is tetratopic and the other two bitopic analogues that can each be viewed as possessing half of the bonding properties of the first. The covalent and supramolecular structures of the silver(I) complexes of tetratopic **L1** and *ortho*-bitopic **L2** are surprisingly similar, where $\pi-\pi$ stacking interactions between the central phenyl rings of the bitopic ligand form a tetratopic unit that acts the same as **L1**. The other noncovalent forces that organize the supramolecular structures are nearly identical, a surprising result given the large differences in the systems. In contrast, the *meta*-bitopic ligand **L3** forms a silver complex with different stoichiometry and structure, although the same types of noncovalent forces organize the supramolecular structure. The differences are driven by the fact that the tris(pyrazolyl)methane units in the sterically hindered *ortho*-ligands **L1** and **L2** prefer κ^2-bonding to silver with the third pyrazolyl ring noncoordinated, yielding a coordination polymer with 2:1 tris(pyrazolyl)methane units/silver metal stoichiometry. In contrast, with less hindered **L3** a structure forms in which each tris(pyrazolyl)methane unit is $\kappa^1-\kappa^2$ bonded to the silvers, a bonding arrangement we have observed previously.[16c,g] In this bonding arrangement all of the pyrazolyl rings are coordinated to a metal, yielding a 1:1 tris(pyrazolyl)methane units/silver stoichiometry. The driving force of strong coordinate covalent bonds, apparently energetically not favored for tris(pyrazolyl)methane units bonded *ortho* on an arene ring, dominates the structural differences.

IR studies support the observations of C−H···π and C−H···F hydrogen bonds in the crystalline samples but not in solution or in the powder samples of **1** and **2**. The importance of the organizational power of C−H···π interactions in these systems is supported by DFT calculations. Despite the fact that solution NMR studies show that the ligand is displaced by acetonitrile but not acetone, the ES-MS of **1** and **2** are similar in both solvents. For **3**, a peak for a bimetallic cation, $[(\mathbf{L3})Ag_2(BF_4)]^+$, is only observed in acetone.

Acknowledgment. The authors thank the National Science Foundation (Grant CHE-0110493) for support. The Bruker CCD single-crystal diffractometer was purchased using funds provided by the NSF Instrumentation for Materials Research Program through Grant DMR 9975623. The NSF (Grant CHE-9601723) and NIH (Grant RR-02425) have supplied funds to support NMR equipment, and the NIH (Grant RR-02849) has supplied funds to support mass spectrometry equipment at the University of South Carolina.

Supporting Information Available: X-ray crystallographic files in CIF format for **L1** and **1**−**3**, a figure with the crystallographic numbering scheme for **L1**, a table with crystallographic data and structure refinement, a table with selected bond lengths and angles, ORTEP diagrams of the asymmetric unit for **1**−**3**, and part of the infrared spectra of **2** in the crystalline and powder states. This material is available free of charge via the Internet at http://pubs.acs.org.

IC034039R